

Supplementary Information

Facile synthesis of $(\text{Ni},\text{Co})@(\text{Ni},\text{Co})_x\text{Fe}_{3-x}\text{O}_4$ core@shell chain structures and $(\text{Ni},\text{Co})@(\text{Ni},\text{Co})_x\text{Fe}_{3-x}\text{O}_4$ /graphene composites with enhanced microwave absorption

Yuan Lin, Lu Xu, Zhiyuan Jiang,* Hongli Li, Zhaoxiong Xie and Lansun Zheng

Department of Chemistry & State Key Laboratory of Physical Chemistry of Solid Surfaces, College of Chemistry and Chemical Engineering, Xiamen University, Xiamen, 361005 China

E-mail: zyjiang@xmu.edu.cn

S1. Experimental Section

Materials

Cobalt(II) acetylacetonate ($\text{Co}(\text{acac})_2$, 98.0%), Nickel(II) acetylacetonate ($\text{Ni}(\text{acac})_2$, 98.0%), Ferric(III) acetylacetonate ($\text{Fe}(\text{acac})_3$, 98.0%) were purchased from Alfa Aesar, a Johnson Matthey Company. Oleylamine (OAm, 80-90%), Oleic acid (OA, 90%), 1-octadecene (ODE, 90%) were obtained from Beijing InnoChem Science & Technology Co., Ltd. N, N-Dimethylformamide (DMF), and ethanol of analytical reagent grade were obtained from Sinopharm Chemical Reagent Company. Graphene was purchased from XFNANO Technology Co., LTD. Distilled water was used in all the experiment.

Preparation of $(\text{Ni},\text{Co})@(\text{Ni},\text{Co})_x\text{Fe}_{3-x}\text{O}_4$ chain structures

Typically, 300 mg $\text{Co}(\text{acac})_2$ (0.0012 mol), 300 mg $\text{Ni}(\text{acac})_2$ (0.0012 mol) and 300 mg $\text{Fe}(\text{acac})_3$ (0.0008 mol) were dissolved in 48.5 mL DMF. 12.0 mL Oleylamine, 8.0 mL 1-octadecene and 1.5 mL Oleic acid were added to the solution till total volume 70.0 mL. The mixed solution was transferred to a 100 mL Teflon-lined stainless-steel autoclave. The sealed vessel was then heated at 180 °C for 24 h before it was cooled to room temperature. The black precipitate was collected by centrifugation and washed with ethanol three times. The final products were obtained via an oxidation process by heating the washed precipitate at 350 °C for 2 h in ambient atmosphere.

Preparation of $\text{Co}@(\text{Co})_x\text{Fe}_{3-x}\text{O}_4$, $\text{Ni}@(\text{Ni})_x\text{Fe}_{3-x}\text{O}_4$ and $(\text{Co},\text{Ni})@(\text{Ni},\text{Co})_x\text{Fe}_{3-x}\text{O}_4$

The preparation process was similar to that of $(\text{Ni},\text{Co})@(\text{Ni},\text{Co})_x\text{Fe}_{3-x}\text{O}_4$, the difference was the feeding precursors. For $\text{Co}@(\text{Co})_x\text{Fe}_{3-x}\text{O}_4$, 600 mg $\text{Co}(\text{acac})_2$ (0.0024 mol) and 300 mg $\text{Fe}(\text{acac})_3$ (0.0008 mol) were dissolved in 48.5 mL DMF. For $\text{Ni}@(\text{Ni})_x\text{Fe}_{3-x}\text{O}_4$, 600 mg $\text{Ni}(\text{acac})_2$ (0.0024 mol) and 300 mg $\text{Fe}(\text{acac})_3$ (0.0008 mol) were employed. For $(\text{Co},\text{Ni})@(\text{Ni},\text{Co})_x\text{Fe}_{3-x}\text{O}_4$, 600 mg $\text{Ni}(\text{acac})_2$ (0.0024 mol) and 200 mg $\text{Co}(\text{acac})_2$ (0.0008 mol) were employed. For each of these solvents, 12.0 mL Oleylamine, 8.0 mL 1-octadecene and 1.5 mL Oleic acid

were added to the solution till total volume 70.0 mL. The mixed solution was transferred to a 100 mL Teflon-lined stainless-steel autoclave. The sealed vessel was then heated at 180 °C for 24 h before it was cooled to room temperature. The black precipitate was collected by centrifugation and washed with ethanol three times. The final products were obtained via an oxidation process by heating the washed precipitate at 350 °C for 2 h in ambient atmosphere.

Preparation of (Ni,Co)@(Ni,Co)_xFe_{3-x}O₄/graphene composites

Typically, (Ni,Co)@(Ni,Co)_xFe_{3-x}O₄ (97mg) and graphene (3mg) were dispersed in ethanol and sonicated for 0.5 h. The black precipitates were isolated by centrifugation, washed with absolute ethanol and finally dried at 70 °C for 8 h.

Characterization

X-ray diffraction (XRD) investigations were performed on Rigaku Ultima IV XRD with Cu K α radiation. The morphology of the products was investigated using scanning electron microscopy (SEM, Zeiss Sigma, 20kV) and transmission electron microscopy (TEM, Philips, Tecnai, F20, 200kV, F30, 300kV). Elemental mapping images were performed with an Energy Dispersive X-ray Detector (EDX) system attached to TEM. For TEM-EDX analysis, the samples were dispersed on carbon coated two-layer copper grid. X-ray photoelectron spectroscopy (XPS) analysis was performed on PHI Quantum 2000. The magnetic characterization of samples was measured by a vibrating sample magnetometer (VSM, Lake Shore).

Electromagnetic measurements

The (Ni,Co)@(Ni,Co)_xFe_{3-x}O₄ hybrid structures based sample (Sample I) was prepared by uniformly mixing of (Ni,Co)@(Ni,Co)_xFe_{3-x}O₄ (50 mg) with paraffin matrix (50 mg). The (Ni,Co)@(Ni,Co)_xFe_{3-x}O₄/graphene based sample (Sample II) was prepared by uniformly mixing (Ni,Co)@(Ni,Co)_xFe_{3-x}O₄/graphene (50 mg) and paraffin matrix (50 mg). The mixture was compressed into a ring sample ($\Phi_{out} = 7.00$ mm and $\Phi_{in} = 3.00$ mm), and the spreading thickness was about 2.0 mm. The relative complex permittivity and permeability were measured by using an Agilent vector network analyzer (85071E) from 2-18 GHz, each 0.08 GHz surveys data.

Similarly, the graphene based sample was prepared by uniformly mixing graphene (1.5 mg) and paraffin matrix (98.5 mg); the Ni@Ni_xFe_{3-x}O₄ based sample was prepared by uniformly mixing Ni@Ni_xFe_{3-x}O₄ (50 mg) and paraffin matrix (50 mg). The Co@Co_xFe_{3-x}O₄ based sample was prepared by uniformly mixing Co@Co_xFe_{3-x}O₄ (50 mg) and paraffin matrix (50 mg). The (Co,Ni)@Ni_xCo_{3-x}O₄ based sample was prepared by uniformly mixing of (Co,Ni)@Ni_xCo_{3-x}O₄ (50 mg) with a paraffin matrix(50 mg). Each of these mixture was compressed into ring sample ($\Phi_{out} = 7.00$ mm and $\Phi_{in} = 3.00$ mm). The relative complex permittivity and permeability were measured by using an Agilent vector network analyzer (85071E) from 2-18 GHz, each 0.08 GHz surveys data.

S2. Supplementary Results

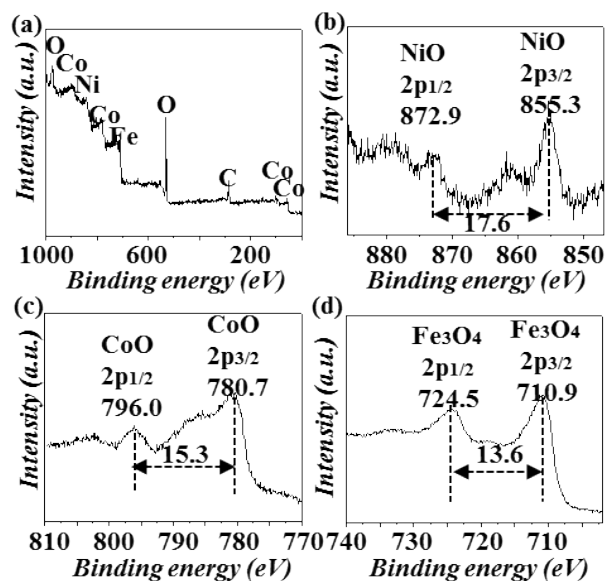


Figure S1 XPS spectra of (a) survey scan, (b) Ni 2p spectrum, (c) Co 2p spectrum and (d) Fe 2p spectrum of $(\text{Ni,Co})@(\text{Ni,Co})_x\text{Fe}_{3-x}\text{O}_4$ chain structures.

The element component of $(\text{Ni,Co})@(\text{Ni,Co})_x\text{Fe}_{3-x}\text{O}_4$ core@shell chain structures was identified by X-ray photoelectron spectroscopy (XPS) (Figure S1). The general XPS spectrum (Figure S1a) for $(\text{Ni,Co})@(\text{Ni,Co})_x\text{Fe}_{3-x}\text{O}_4$ chains shows photoelectron lines at a binding energy of 710.9, 780.7 and 855.3 eV completely composed of Fe in Fe_3O_4 2p_{3/2}, Co in CoO 2p_{3/2}, and Ni in NiO 2p_{3/2}, respectively. Figure S1b-1d detail the high resolution spectra of Fe, Co and Ni. In Figure S1b, the binding energy peaks at 855.3 and 872.9 eV correspond to Ni in NiO 2p_{3/2} and 2p_{1/2}, suggesting the existence of NiO. In Figure S1c, the Co 2p_{1/2} (796.0 eV) and Co2p_{3/2} (780.7 eV) peaks suggest that Co exists as CoO. In Figure S1d, the binding energy at 724.5 eV and 710.9 eV are the characteristic doublets of Fe_3O_4 2p_{3/2} and Fe_3O_4 2p_{1/2} in samples. The corresponding satellite peak located at 710.9 eV can be attributed to the presence of Fe (III) ions in Fe_3O_4 . The peaks correspond to Ni⁰ and Co⁰ is hardly observed in XPS spectra of as prepared products, which may be caused by the existence of thick metal oxides shell layer and the XPS only collect the electrons come from the surface less than dozens nanometers.

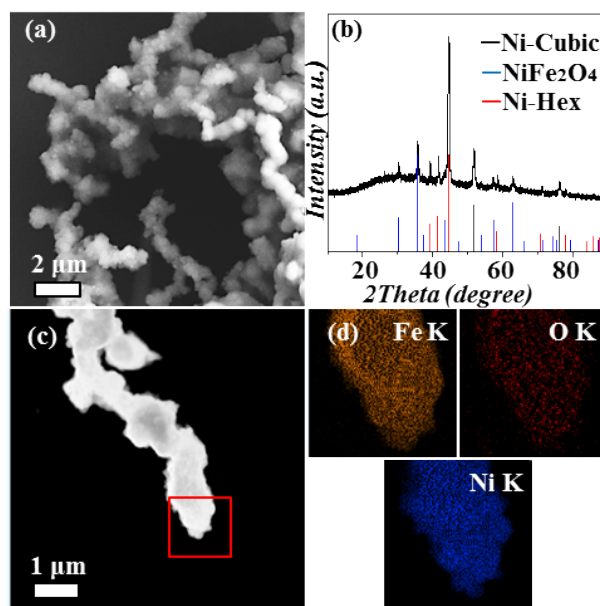


Figure S2 (a) SEM image, (b) XRD pattern, (c) the HAADF image and (d) the mapping images of Ni@Ni_xFe_{3-x}O₄.

Figure S2a shows a typical SEM image of the Ni@Ni_xFe_{3-x}O₄ hybrid structures. It can be clearly seen that most of the products have chain structures. The XRD pattern (Figure S2b) can be indexed by three sets of diffraction peaks. The diffraction peaks located on 30.2°, 35.6° are corresponding to (220), (311) crystal plane of cubic NiFe₂O₄ (PDF No.00-010-0325). The diffraction peaks on 44.4°, 51.6° and 76.1° can be assigned to cubic Ni (PDF No. 00-001-1258). The diffraction peaks on 39.1°, 41.5° and 44.5° can be indexed as hexagonal Ni (PDF No. 00-045-1027). From the EDX mapping images (Figure S2d), it can be clearly observed that the element O is mainly located on the outer layer. In the center of the chain structure, element Ni has a stronger contrast than element Fe. These results reveal that as prepared products are Ni@Ni_xFe_{3-x}O₄ core@shell chain structures.

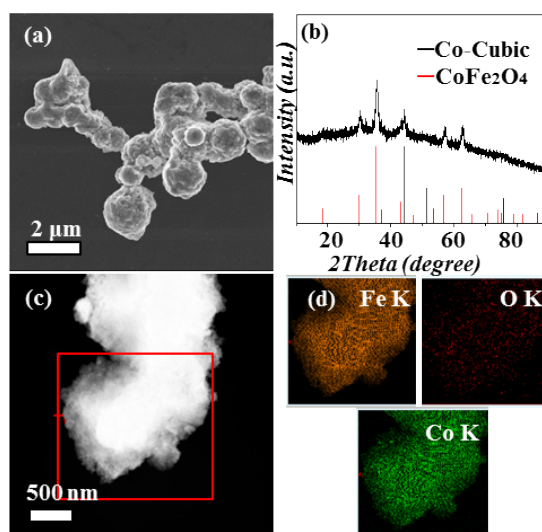


Figure S3 (a) SEM image, (b) XRD pattern, (c) the HAADF image and (d) the mapping images of Co@Co_xFe_{3-x}O₄.

Figure S3a shows the typical morphologies of the $\text{Co}@_{\text{Co}_x\text{Fe}_{3-x}\text{O}_4}$ hybrid structures. The XRD (Figure S3b) analysis shows that Co and $\text{Co}_x\text{Fe}_{3-x}\text{O}_4$ are co-presented in the products. Further detail information was provided by HAADF and EDX mapping images (Figure S3c, 3d), which suggest that the products are mainly $\text{Co}@_{\text{Co}_x\text{Fe}_{3-x}\text{O}_4}$ structures.

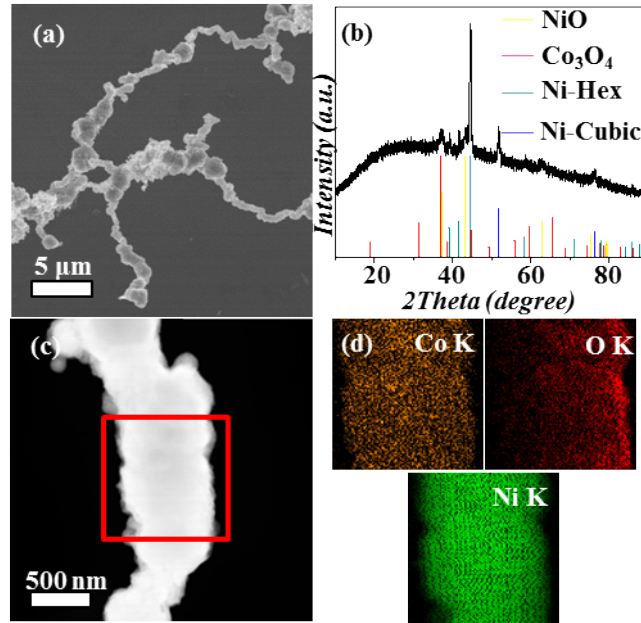


Figure S4 (a) SEM image, (b) XRD pattern, (c) the HAADF image, (d) the elemental maps of $(\text{Ni,Co})@_{\text{Ni}_x\text{Co}_{3-x}\text{O}_4}$.

The low magnification SEM image (Figure S4a) indicates that most of the products have chain structures. In the XRD patterns (Figure S4b), the diffraction peaks located on 31.3° , 36.9° and small peaks at 37.2° , 43.2° and 62.8° can be assigned to cubic Co_3O_4 (PDF No. 03-065-3103) and cubic NiO (PDF No. 00-044-1159), respectively. Other peaks can be indexed as hexagonal Ni (PDF No. 00-045-1027), cubic Ni (PDF No. 00-001-1258) or Co (PDF No. 00-001-1255) from their similar structure and cell parameters. Definite compositional information was provided by HAADF and EDX mapping images (Figure S4c, 4d). The EDX mapping analysis illustrates that the Ni element concentrates inside while the Co element spreads over the surface. The distribution of O is almost coincided with that of Co elements and obvious enrichment in the outer layer. These results suggest that the products are mainly $(\text{Ni,Co})@_{\text{Ni}_x\text{Co}_{3-x}\text{O}_4}$ hybrid structures.

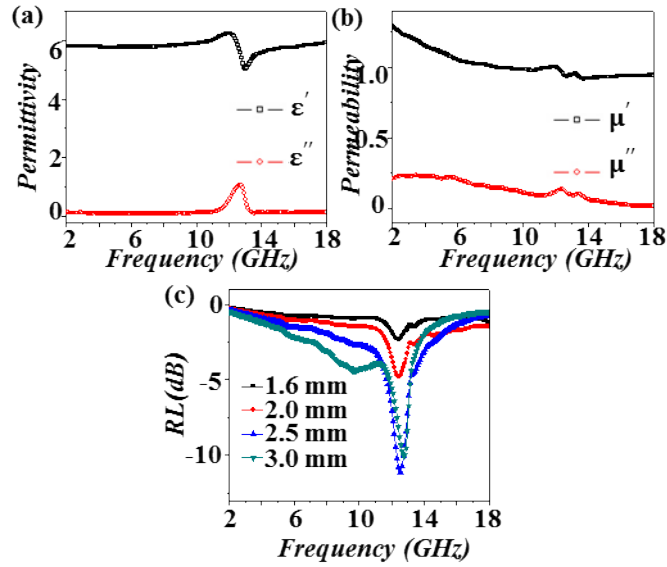


Figure S5 (a) The effective complex permittivity, (b) complex permeability and (c) electromagnetic wave absorption performance of Ni@Ni_xFe_{3-x}O₄.

Figure S5 shows the complex parameters and RL value of Ni@Ni_xFe_{3-x}O₄. The highest ϵ' value is 6.21 at 12.16 GHz and the highest ϵ'' value is about 1.06 at 12.72 GHz. The μ' value of the sample declines quickly from 1.28 to 0.91 and μ'' value is stable decreased from 0.21 to 0.02. The strongest RL of Ni@Ni_xFe_{3-x}O₄ based sample is -11.16 dB at 12.48 GHz with the thickness of 2.5 mm. At the thickness of 2.0 mm, the strongest RL of Ni@Ni_xFe_{3-x}O₄ is -4.81 dB at 12.4 GHz.

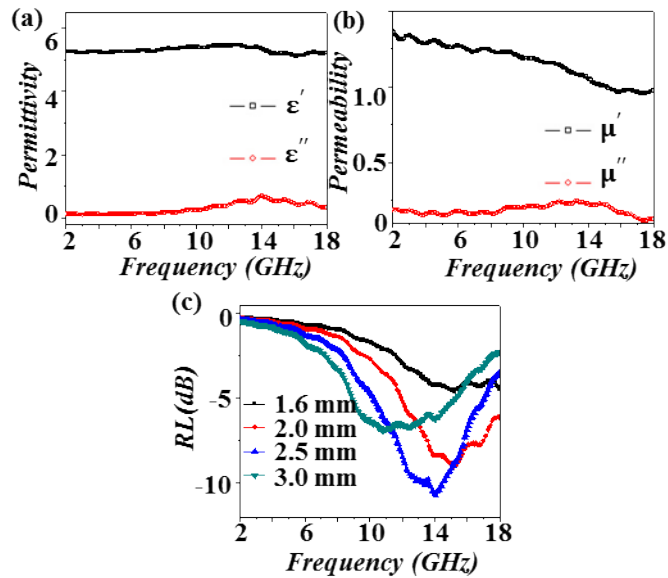


Figure S6 (a) The effective complex permittivity, (b) complex permeability and (c) electromagnetic wave absorption performance of Co@Co_xFe_{3-x}O₄.

The complex parameters and RL value of $\text{Co}@\text{Co}_x\text{Fe}_{3-x}\text{O}_4$ is shown in Figure S6. The highest ϵ' value of $\text{Co}/\text{Co}_x\text{Fe}_{3-x}\text{O}_4$ is about 5.42. The μ' value dropped quickly from 1.36 to 0.95 and μ'' value is stable from 0.23 to 0.11. The strongest RL of $\text{Co}/\text{Co}_x\text{Fe}_{3-x}\text{O}_4$ is -10.50 dB observed at 13.92 GHz with a thickness of 2.5 mm. At the thickness of 2.0 mm, the strongest RL of the sample is -8.97 dB at 15.36 GHz.

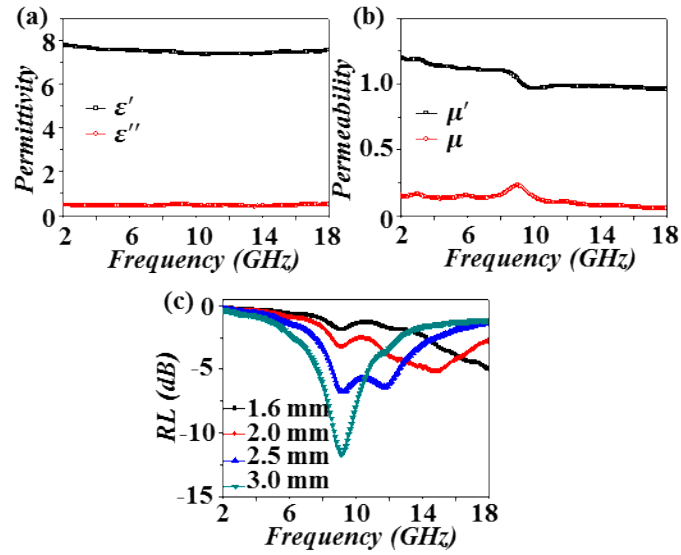


Figure S7 (a) The effective complex permittivity, (b) complex permeability and (c) electromagnetic wave absorption performance of $(\text{Ni,Co})@\text{Ni}_x\text{Co}_{3-x}\text{O}_4$.

Figure S7 shows the complex parameters and RL value of $(\text{Ni,Co})@\text{Ni}_x\text{Co}_{3-x}\text{O}_4$. The highest ϵ' value of $(\text{Ni,Co})@\text{Ni}_x\text{Co}_{3-x}\text{O}_4$ is about 7.70. The μ' value declines quickly from 1.19 to 0.97 and μ'' value is stable from 0.22 to 0.05. The strongest RL of $(\text{Ni,Co})@\text{Ni}_x\text{Co}_{3-x}\text{O}_4$ is -11.59 dB at 9.28 GHz with the thickness of 3.0 mm.

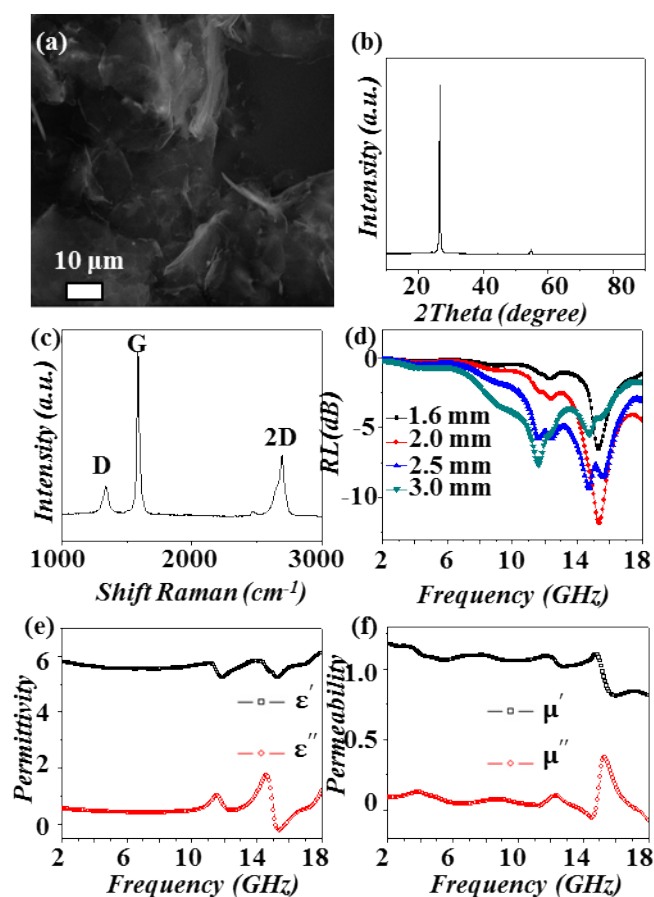


Figure S8 (a) SEM image, (b) XRD pattern and (c) Raman spectrum of graphene; (d) Frequency dependence of the calculated reflection loss, (e) the effective complex permittivity and (f) the complex permeability value of graphene.

The SEM image and XRD patterns of pure graphene are shown in Figure S8a and S8b. It can be seen that the pure graphene shows a slight diffraction peak at 2θ of ca. 26.6° . The graphene can also be confirmed by the Raman spectra (Figure S8c). The intense feature around 1326 , 1574 , 2686 cm^{-1} is the characteristic bands of D, G and 2D bands. As shown in Figure S8d, the maximum RL value of the graphene is -11.84 dB at 15.36 GHz with 2 mm. The highest ϵ' value and ϵ'' value of graphene is about 5.80 at 13.92 GHz and 1.72 at 14.56 GHz, respectively. The largest μ' value and μ'' value of graphene is about 1.17 at 2.16 GHz and 0.37 at 15.28 GHz, respectively.

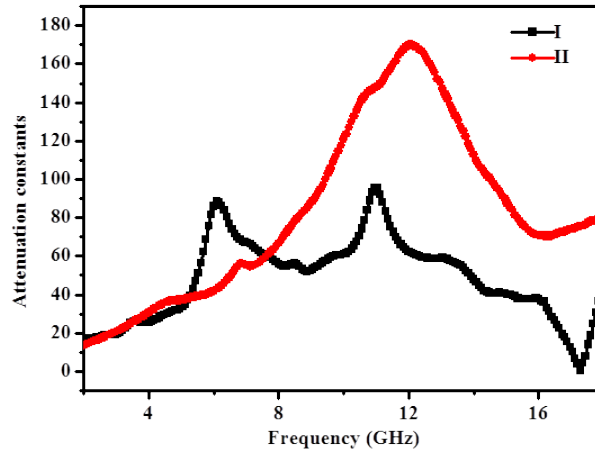


Figure S9 Attenuation constant– frequency (α -f) curves of $(\text{Ni},\text{Co})@(\text{Ni},\text{Co})_x\text{Fe}_{3-x}\text{O}_4$ (sample I) and $(\text{Ni},\text{Co})@(\text{Ni},\text{Co})_x\text{Fe}_{3-x}\text{O}_4/\text{graphene}$ (sample II).

Attenuation constants in the interior absorber can be expressed by¹⁻³

$$\alpha = \frac{\sqrt{2}\pi f}{c} \sqrt{(\mu''\varepsilon'' - \mu'\varepsilon') + \sqrt{(\mu''\varepsilon'' - \mu'\varepsilon')^2 + (\mu'\varepsilon'' + \mu''\varepsilon')^2}}$$

where c is the velocity of light. From the above equation, it is noted that high values of μ'' and ε'' would result in high α value. In our case, the μ'' value of $(\text{Ni},\text{Co})@(\text{Ni},\text{Co})_x\text{Fe}_{3-x}\text{O}_4/\text{graphene}$ is higher than that of the $(\text{Ni},\text{Co})@(\text{Ni},\text{Co})_x\text{Fe}_{3-x}\text{O}_4$ from 7.44 GHz to 18.0 GHz, and ε'' value of $(\text{Ni},\text{Co})@(\text{Ni},\text{Co})_x\text{Fe}_{3-x}\text{O}_4/\text{graphene}$ is also higher than that of the $(\text{Ni},\text{Co})@(\text{Ni},\text{Co})_x\text{Fe}_{3-x}\text{O}_4$ from 9.28 GHz to 13.68 GHz. Therefore, the sample $(\text{Ni},\text{Co})@(\text{Ni},\text{Co})_x\text{Fe}_{3-x}\text{O}_4/\text{graphene}$ composites possess bigger α in frequency range from 7.68-18 GHz. The high α indicated that the $(\text{Ni},\text{Co})@(\text{Ni},\text{Co})_x\text{Fe}_{3-x}\text{O}_4/\text{graphene}$ composites have enhanced dielectric loss and magnetic loss and result in excellent microwave absorption in high frequency range.

1. B. Lu, H. Huang, X. L. Dong, X. F. Zhang, J. P. Lei, J. P. Sun and C. Dong, *J. Appl. Phys.*, 2008, **104**, 114313.
2. S. L. Wen, Y. Liu, X. C. Zhao, J. W. Cheng and H. Li, *Phys. Chem. Chem. Phys.*, 2014, **16**, 18333.
3. B. Zhao, G. Shao, B. B. Fan, W. Y. Zhao and R. Zhang, *Phys. Chem. Chem. Phys.*, 2015, **17**, 2531.